DFT study of $[Pt(Cl)_2L]$ complex (L= rubeanic acid) and its derived compounds with DNA purine bases

Amit Kumar[1], Gianluca Gatto[1], Francesco Delogu[2] and Luca Pilia[2*]

[1] Department of Electrical and Electronic Engineering, University of Cagliari, via Marengo 2, 09123 Cagliari, Italy

[2] Department of Mechanical, Chemical and Materials Engineering, University of Cagliari, via Marengo 2, 09123 Cagliari, Italy

*Corresponding Author

Email: pilialuc@unica.it

Phone: +39-070-6755051

Abstract

In this study, we present a systematic computational investigation on the electronic properties of cisplatin (cis-$[Pt(Cl)_2(NH_3)_2]$ (CP) and complex $[Pt(Cl)_2L]$ (**1**) (L= rubeanic acid) employing all-electron density functional theory. In detail, we analyzed essential molecular properties such as geometrical parameters, ionization energies, electron affinity, highest occupied molecular orbital, and lowest unoccupied molecular orbital energies. Concerning CP, molecule **1** exhibited improved lipophilicity and a pronounced electrophilic property. Furthermore, to investigate and compare the DNA binding capability between CP and molecule **1,** we extended the investigation to the guanine and adenine derived complexes, respectively. Complexes of molecule **1** with the adenine and guanine bases followed a similar trend of stability found for CP systems, with the highest affinity found for guanine complexes. Altogether, molecule **1** displayed promising physicochemical and druglikeness features to serve as a starting point for developing a drug-like enough that could be therapeutically useful.

Keywords

Cisplatin, Rubeanic acid, Density Functional Theory, Electronic properties, Drug design

1 INTRODUCTION

Cisplatin (CP), along with other Pt(II)-based complexes, is one of the most widely prescribed drugs for treating patients with cancer [1]. Unfortunately, in addition to its antineoplastic activity against several tumors, CP presents also significant side effects among which gastrointestinal symptoms, nephrotoxicity, neuropathy, ototoxicity, and myelosuppression [2, 3]. Moreover, its effectiveness as an anticancer drug can also be reduced because of the occurrence of cross-resistance to the treatment [4].

Some of the CP side-effects, such as nephrotoxicity, have been suggested to be related to the interaction of Pt(II) ion with sulfur-containing enzymes[5, 6]. Furthermore, some of the mechanisms proposed to explain CP inactivation are also related to interaction with protein and nonprotein containing thiols [7, 8]. Taking into account the hard and soft acids and bases (HASB) theory [9], the affinity between Pt(II) sulfur bearing ligands can be explained considering their common *soft* feature. Moreover, the π back-bonding donation from the metal center to empty orbitals at the sulfur atoms (π acceptors) may make more stable the S-Pt interaction. Also, atoms with π acceptor property bound directly to the metal center should make less favorable the further formation of bonds between Pt and other atoms with the same capability, and therefore may reduce the interaction of the drug with sulfur-containing proteins.

With an aim to tackle the above problems, molecules containing thiol or thiocarbonyl groups have been studied as chemoprotective drugs [6, 10-13]. More recently, several Pt complexes of chelating ligands with sulfurs as donor atom, which have been suggested to be able to shield the metal center from interactions with sulfur-containing enzymes, have been proposed

as anticancer drugs [5, 14]. In particular, dithiocarbamate molecules are effective at reducing the toxicity of CP when administered as antidote[14]. Moreover, Pt(II) complexes with dithiocarbamate as ligand display not only good antineoplastic activity but also lower toxicity compared to CP [5, 14].

In the early seventies, Cleare and Hoeschele proposed a structural-anticancer activity relationship for platinum (Pt) complexes with general formula PtL_2X_2 [15]. In particular, they suggested that a Pt(II) or Pt(IV) compound to be active as anti-tumor drug must have: i) neutral charge; ii) not strongly bound leaving groups in *cis* positions; iii) at least one hydrogen atom bound to aminic nitrogen. However, in the nineties [16], it has been demonstrated that neutral charge of the complex is not an indispensable feature for anti-cancer activity. Thus, considering these structural features, it motivated us to investigate the Pt(II) dichloro-complex with the rubeanic acid (RA) as a non-leaving ligand (see chart 1) as a model system suitable for designing prospective anticancer drugs with an improved uptake and lower toxicity.

This complex presents indeed, all the requirements listed above for an anti-cancer Pt drug. Moreover, the chelating capability of the non-leaving group increases the stability of the compound [5]. Besides, the presence of sulfur atoms directly bound to the Pt ion could reduce the drug affinity to cysteine or other sulfur-containing proteins, potentially decreasing the toxicity and increasing the activity of the complex, as mentioned above.

Several computational studies have provided useful insights into the structure of cisplatin, its hydrolysis and comparison of its binding to the purine bases [17-21]. In this paper, we present a detailed computational investigation employing density functional theory (DFT) [22] for compound **1** and compare its molecular properties with CP complex. Furthermore, to study the capability of compound **1** to form a chemical bond with the nucleobases of DNA,

complexes derived from **1** with guanine and adenine have been considered along with the corresponding compounds from CP.

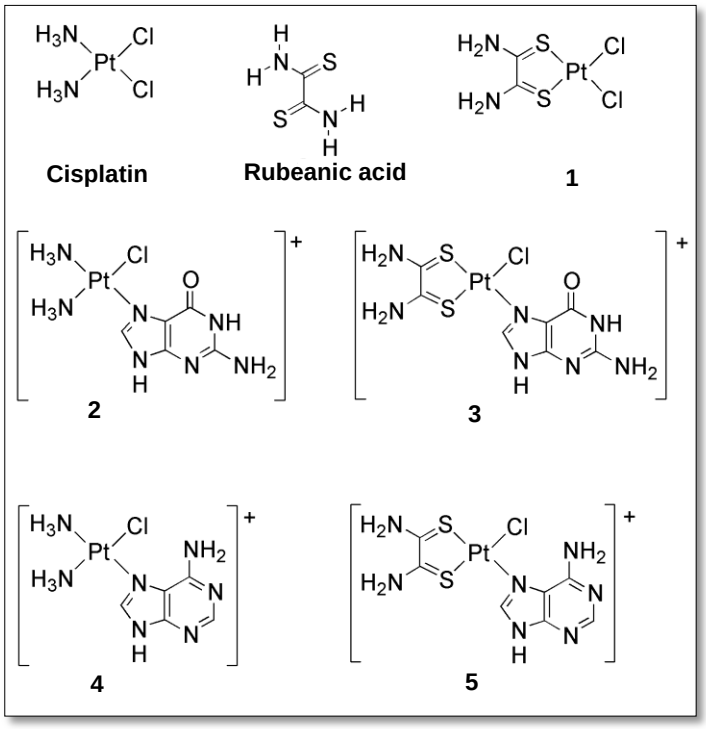

Chart 1. Molecules under investigation (see text).

2. COMPUTATIONAL METHODS

The molecules under investigation were drawn using Marvin[23]. Two-dimensional structures were then converted to three-dimensional structures using open babel software[24]. The ground-state geometry of all seven molecules depicted in chart 1 has been optimized by DFT methods[22] at B3LYP [25, 26] level of theory, using both *Gaussian 09* [27] and *NWChem* [28] programs. Basis sets 6-31G* and 6-311+G(d,p) were used for atoms C, H, O, N, S, Cl, and LANL2DZ ECP basis set [29] on Pt.

No significant differences in the geometry of the molecules were observed between the two basis sets and the two methods. On the derived geometry optimized structures, quantum chemical parameters such as the lowest unoccupied molecular orbital (E_{LUMO}) and the highest occupied molecular orbital (E_{HOMO}) were then obtained from the optimized structures. The energy difference between E_{HOMO} and E_{LUMO} were then used to calculate electronic chemical potential (μ) and chemical hardness (η) as follows:

$$\boldsymbol{\mu = \frac{E_{HOMO}+E_{LUMO}}{2}} \quad \textbf{(1)}$$

$$\boldsymbol{\eta = \frac{E_{HOMO}-E_{LUMO}}{2}} \quad \textbf{(2)}$$

The difference in the total energy between the neutral and the anion radical in the optimized geometry of the neutral form was calculated to obtain the vertical electron affinity (EA_V). While the difference in the total energy between the cation radical and the neutral molecule in the optimized geometry of the neutral molecule were used to calculate vertical ionization energy (IE_V)[30]. The fundamental gap ($E_{\mathbf{GAP}}$) was calculated as defined in the ΔSCF scheme [31-34] as:

$$E_{\mathbf{GAP}} = IE_V - EA_V \quad \textbf{(3)}$$

In order to evaluate the effect of the solvent on the molecular properties, the Polarizable Continuum Model (PCM) was employed to optimize the ground state geometry of molecules **RA**, **1**, **3** and **5** in a water simulated electric field. Both 6-31G* and 6-311+G(d,p) were used as basis set for atoms C, H, O, N, S, Cl, whereas LANL2DZ ECP basis set was employed for the Pt(II) ion.

3. RESULTS AND DISCUSSION

3.1 Physicochemical and biological properties

Physicochemical and biological properties for the molecules (Table 1), which are considered necessary in modern computer-aided drug design (CADD)[35, 36] were analyzed using SwissADME web tool [37]. Lipophilicity is considered as an essential element in drug design [38], which has been recognized to influence cellular drug uptake [39, 40]. While the flexibility of a molecule can be related to the number of rotatable bonds, the higher the number more flexible is the molecule.

Table 1. Evaluated physicochemical properties.

Properties	**CP**	**RA**	**1**	**2**	**3**	**4**	**5**
Num. Atoms	11	10	13	26	28	25	27
Molecular Weight (g/mol)	300.05	120.20	386.18	415.72	501.85	399.72	485.85
Molecular Refractivity	21.16	32.72	44.43	54.22	77.49	51.40	74.67
Num. H-bond acceptor	4	0	0	2	2	2	2
Num. H-bond donor	2	2	2	4	5	4	4
Num. Rotatable bonds	0	1	0	1	1	1	1
Polar surface area ($Å^2$)	6.48	116.22	116.22	98.97	208.71	79.00	188.74
Lipophilicity index (LogP)	-2.21*	-0.44	0.94	0.57	-0.52	1.28	0.19
Water solubility	Soluble	Moderate Soluble	Soluble	Soluble	Moderate Soluble	Soluble	Soluble
Druglikeness	Yes	Yes	Yes	Yes	Yes	Yes	Yes

*from ref. [41]

Together with five new compounds, for completeness, we also report the physicochemical properties of CP (commonly used chemotherapy drugs) and RA (used as chelating and thiolating agent).

Among the five new compounds considered, molecule **1** possess the lowest number of atoms and **3** the highest number of atoms. Molecule **1** is a Pt complex formed with RA as a non-

leaving group and a similar leaving group as CP. Molecule **2** and **4** are Pt(II) –DNA compounds with NH_3 as a non-leaving group, while in **3** and **5** the non-leaving group in RA. Molecule **3** has the highest molecular weight and molecular refractivity. Among the five compounds, the Pt(II)–DNA compounds (**2**, **3**, **4** and **5**) possess two H-bond acceptor atoms each, while absent in **1**. Molecules **2**, **4** and **5** share a similar H-bond donating capability, while **3** has the highest H-bond donating capability and **1** the lowest. The Pt(II)-DNA compounds (**2, 3, 4** and **5**) displayed similar molecular flexibility reflected from the same number of rotatable bonds, while **1** displayed the lowest flexibility. Polar surface area (PSA) is an essential chemical descriptor that has been shown to correlate well with passive molecular transport properties of molecules through membranes [42]. In a previous study [43] authors examined a set of 1100 drug candidates and used the metabolism data collected from rats to understand the correlation between the bioavailability of a compound and physicochemical properties. Notably, the same authors established that compounds with less than 10 rotatable bonds together with a polar surface area <140 $Å^2$ emerged as candidates with good oral bioavailability. Among the five compounds in the present study, the number of rotatable bonds and the PSA value of molecules **1**, **2,** and **4** lies within the acceptable range of good orally bioavailable candidates. The most lipophilic compound is **4**, and the sequence order among the compounds is as follows **4** > **1** > **2** > **5** > **3**. A recent breakdown in new drug development has been attributed to poor water solubility, thus suggesting its essential role in the development of a candidate drug molecule [44]. In general, the five compounds investigated here displayed moderate to good water solubility characteristics [45]. The druglikeness, which is a qualitative concept in drug design, was examined for the molecules using the Lipinski's rule of five [46]. All the compounds displayed druglikeness

characteristics, with an only exception being molecule **3** that displayed one violation (MW >500 g/mol, Table 1).

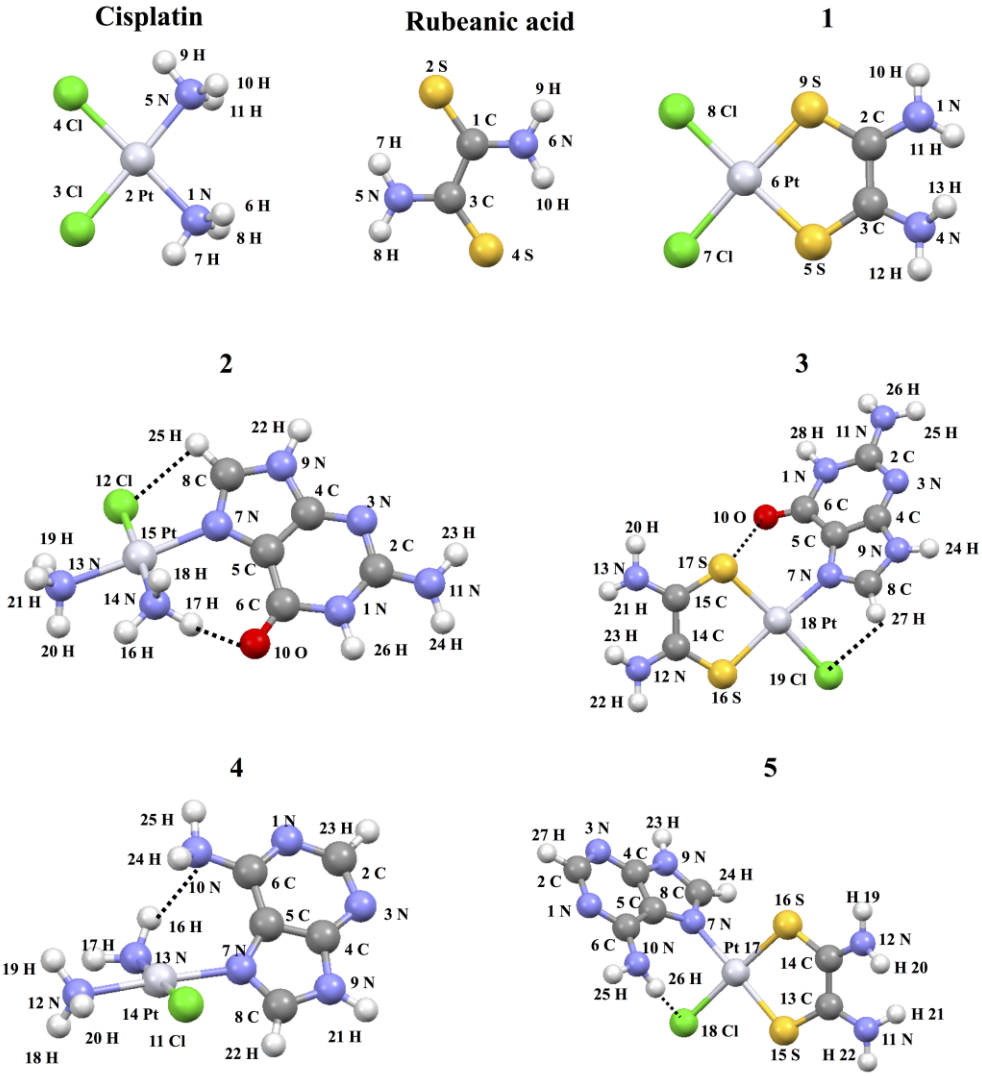

Fig. 1 Optimized geometry of the investigated molecules obtained using the DFT method at B3LYP/6-31+G* level of theory. Dashed lines represent distances shorter than the sum of the Van der Waal radii.

3.2 Optimized geometry, frontier orbitals, and electrostatic potentials

All the complexes (Fig. 1) present the four donor atoms and the metal center lying on the same plane in a square planar coordination geometry, with maximum displacements from the plane ranging from 0 (CP and RA) to 0.061 Å for **5** (Fig.s S1-S3). The distances Pt-N_{base}

(Tables 2, S4 and S5) calculated for complexes **2** and **3** are quite similar (2.058 and 2.069 Å respectively) suggesting similar interactions between the metal center and the nucleobase in the two complexes. Analogous thought can be done for the compounds with the adenine (**4** and **5**; see Tables 2, S6 and S7). No significant differences have been observed between the inter-atomic distances calculated with the basis sets 6-31G* and 6-311+G(d,p) as well as between those predicted in gas-phase and water (see Tables S2, S3, S5 and S7).

Table 2. Key inter-atomic distances and binding energy of molecules under investigation.

Compound	Pt-Cl (Å)	Pt-N (Å)	Pt-S (Å)	Pt-N_{base} (Å)	C-S (Å)	C-C (Å)	C-N (Å)	Binding energy (kca/mol)
CP	2.348	2.115	–	–	–	–	–	–
RA	–	–	–	–	1.672	1.534	1.332	–
1	2.342	–	2.324	–	1.686	1.462	1.366	–
2	2.354	2.089[a]/ 2.108	–	2.058	–	–	–	79.25 (80.45)[b]
3	2.350	–	2.328[a]/ 2.347	2.069	1.679[a]/ 1.687	1.481	1.354[a]/ 1.344	60.41
4	2.322	2.095[a]/ 2.127	–	2.049	–	–	–	64.02 (65.51)[b]
5	2.346	–	2.335[a]/ 2.350	2.060	1.687[a]/ 1.687	1.487	1.343	50.83

[a] due to lack of molecular symmetry two bond distances are present. [b] from ref. [47]

The binding energy estimation [48] for molecules **2–5** was performed by subtracting the sum of the individual energy of the fragments from that of the corresponding complex, employing DFT calculations (in Table 2), which indicated complex **2** to be much favored over complex **3** by ca. 19 kcal/mol, while compound **4** to be much preferred over complex **5** by ca. 13 kcal/mol. Thus, suggesting CP to form more stable complexes than those built with molecule **1**. Intramolecular contacts shorter than the sum of van der Waals radii, involving the nucleobase and another ligand, are predicted for compounds **2-5** (see Fig. 1 and Table S8).

These contacts were estimated using both NWCHEM [28] and Gaussian09 [27] programs, and we found a maximum variation of 3% between them. These interactions could play an essential role in stabilizing the drug-DNA compound [47]. In particular, two short intramolecular contacts are present in molecule **2** (Cl···H25 and O···H17) and one each in molecules **3** (S···H25), **4** (N10···H16) and **5** (Cl···H26). Also, the calculated bond distances for all the compounds (Table 3) were found to agree with other previously reported experimental and theoretical studies on similar compounds [49-55].

Table 3. Comparison of inter-atomic distances between the investigated molecules and similar compounds reported in the literature (calculated and ***experimental*** values).

Compound	**Pt-N_{NH3} (Å)**	**Pt-$N_{guanine}$ (Å)**	**Pt-$N_{adenine}$ (Å)**	**O_G...HNH_2[1] (Å)**	**N_A...HNH_2[1] (Å)**
CP*	2.115	–	–	–	–
2*	2.089[2]/ 2.108	2.058	–	1.77	–
4*	2.095[2]/ 2.127	–	2.049	–	2.08
[*cis*-$Pt(NH_3)_2GA]^{2+}$ (HH)[3] [53]	2.089/ 2.095	2.041	2.044	2.01	2.09
[*cis*-$Pt(NH_3)_2GA]^{2+}$ (HT)[3] [53]	2.087/ 2.076	2.058	2.053	1.77	2.06
[*cis*-$Pt(NH_3)_2G_2]^{2+}$ (HH)[3] [53]	2.074	2.065/ 2.065	–	1.84	–
[*cis*-$Pt(NH_3)_2G_2]^{2+}$ (HT)[3] [53]	2.073	2.061/ 2.061	–	1.80	–
[*cis*-$Pt(NH_3)_2GA](NO_3)_2$ (HH)[3] [54]	***2.033/ 2.032***	***2.006***	***2.036***	–	–
[*cis*-$Pt(NH_3)_2G_2]SO_4$ (HH)[3] [55]	***1.970/ 2.047***	***1.962/ 2.010***	**–**	–	–
[*cis*-$Pt(NH_3)_2G_2][Pt(CN)_4]$ (HH)[3] [55]	***2.046/ 2.044***	***2.022/ 2.002***	**–**	–	–

[1] H-bond; [2] due to lack of molecular symmetry two bond distances are present.[3] G = guanine; A = adenine; HH = head-to-head; HT= head-to-tail (mutual orientation of the bases).* This work.

The frontier orbitals (FOs) are depicted in Fig. 2. As one can see in CP, the highest occupied molecular orbital (HOMO) is a π-antibonding out-of-plane combination of *d*-metal orbitals and *p*-orbitals of chloride ligands. The lowest unoccupied molecular orbital (LUMO) is formed by σ^* interactions involving the Pt d_{x2-y2} orbital and the ligands orbitals. In the case of complex **1**, the HOMO has a shape like that of CP, whereas the LUMO is mainly due to a combination of Pt *d* orbitals and the LUMO of RA. As far as the compounds **2**-**5** are concerned, the LUMOs are mainly composed by the corresponding MO of CP (**2** and **4**) or **1** (**3** and **5**) while the HOMOs, for the most part, are formed by the orbitals of the nucleobases, except in the case of complex **4** which shows a HOMO composed by an π^* combination of a *d* metal and the p_z chlorine ligand orbitals. In the case of compound **4,** the MO corresponding to the HOMOs of molecules **2**, **3,** and **5** is the HOMO-1 (see Figure S4).

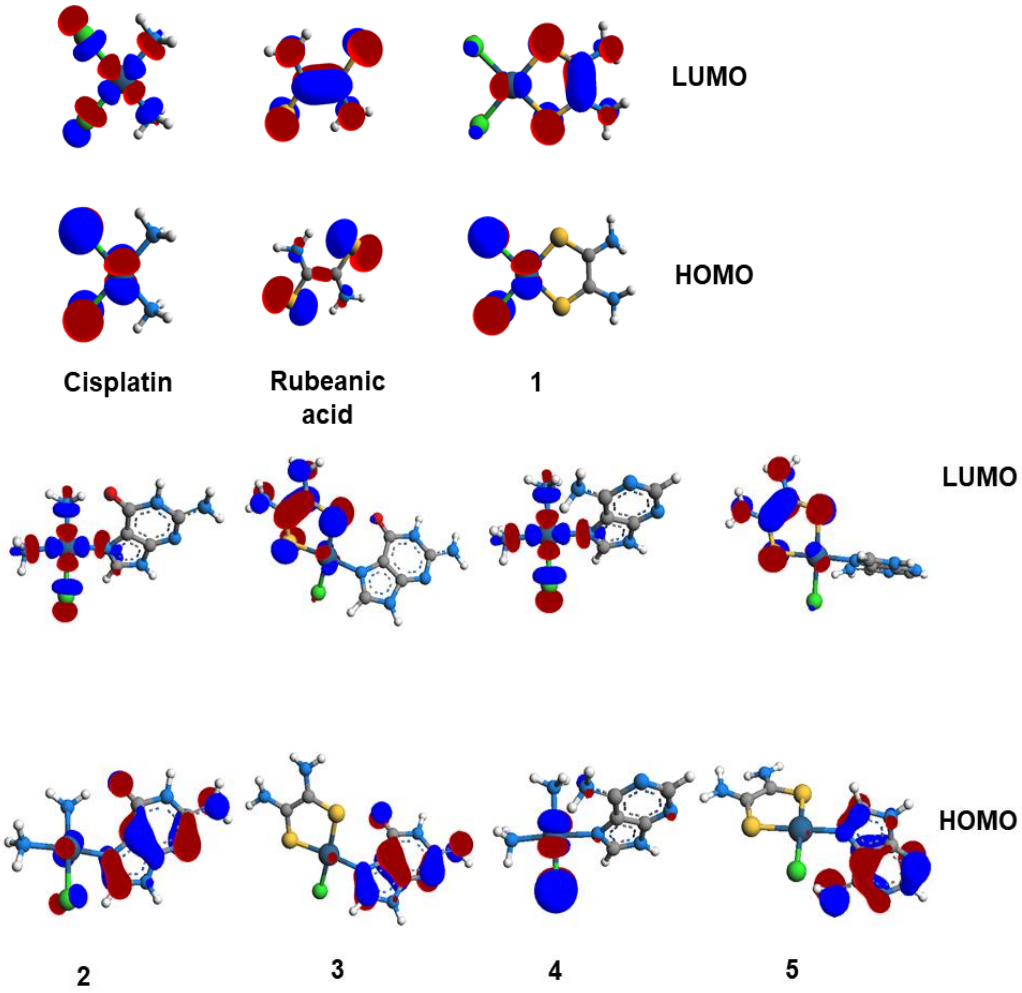

Fig. 2. Frontier molecular orbitals calculated by DFT at B3LYP/6-31+G* level of theory (contour plot 0.04).

Electron densities mapped with the electrostatic potential (EP) of the investigated compounds are shown in Fig.s 3 and 4. As expected, considering the electron-withdrawing capabilities, negative EPs are predicted on chloride ligands complex for CP and **1** complexes, whereas the hydrogen atoms present the most positive values. The positive charge in the complexes **2-5** affects the overall potential distribution, and as expected, no region with negative EPs was predicted for these compounds. The less positive EPs in these molecular ions are localized on chlorine, oxygen, and some nitrogen atoms: 1N in guanine, while 1N and 3N in adenine

containing complexes (Fig. 1), respectively. Moreover, these findings are also in agreement with the observed intramolecular interactions, as discussed above.

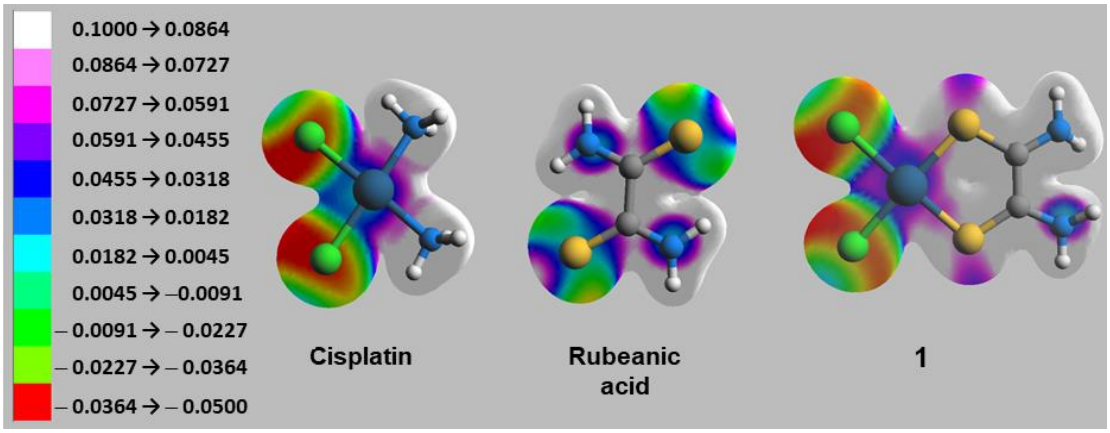

Fig. 3. Electrostatic potentials mapped on electron density isosurfaces for CP, RA, and **1** calculated by DFT (contour plot 0.0002). The colors are assigned following the EP at the point on the isosurface.

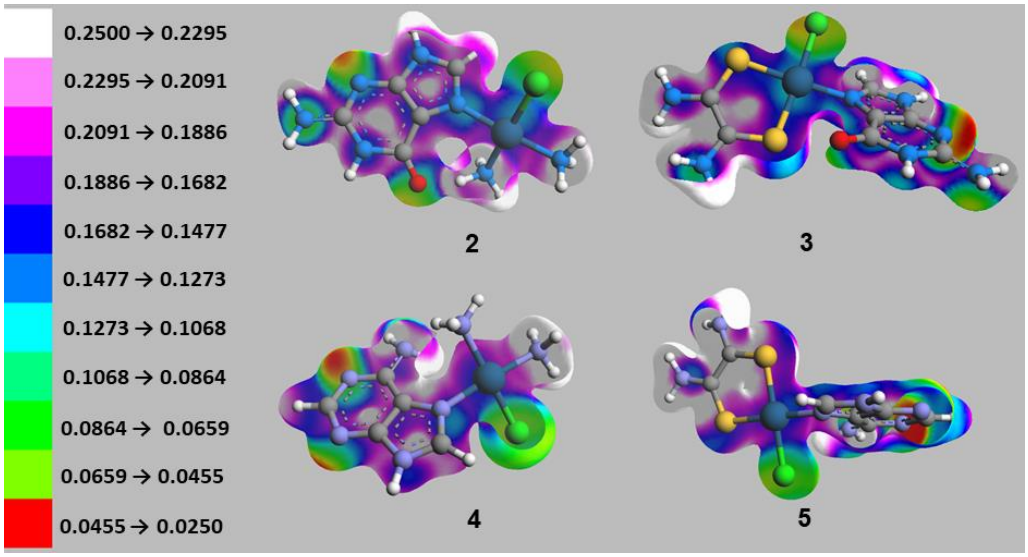

Fig. 4. Electrostatic potentials mapped on electron density isosurfaces for complexes **2**-**5** calculated by DFT (contour plot 0.0002). The colors are assigned following the EP at the point on the isosurface.

3.3 Electronic and molecular properties

The calculated electronic properties of the molecules are reported in Table 4.

Table 4. Electronic and molecular properties of the molecules investigated in this study. The values reported are in electron volt (eV).

	B3LYP/6-31+G* [eV]						
	CP	**RA**	**1**	**2**	**3**	**4**	**5**
$\mathbf{E_{LUMO}}$	-1.60	-2.64	-4.41	-4.54	-6.92	-5.11	-7.55
$\mathbf{E_{HOMO}}$	-6.13	-6.10	-6.34	-9.41	-8.96	10.04	-9.13
$\mathbf{E_{LUMO}–E_{HOMO}}$	4.53	3.46	1.93	4.82	2.04	4.93	1.58
η	2.26	1.73	0.96	2.41	1.02	2.46	0.79
μ	-3.86	-4.37	-5.38	-7.00	-7.94	-7.58	-8.34
$\mathbf{IE_V}$	8.33	8.26	9.80	11.06	10.51	11.78	10.82
$\mathbf{EA_V}$	-0.84	0.60	2.68	2.91	5.25	3.39	5.87

The electron accepting and donating capability of the molecules can be described as LUMO and HOMO, respectively. Molecule **1** displayed a lower value of E_{LUMO} compared to CP, thus a better electron-accepting ability. Among the Pt(II)-DNA complexes, molecule **5** showed the lowest E_{LUMO} -7.55 eV, while **2** the highest. Concerning HOMO, molecule **1** displayed the highest E_{HOMO} of -6.34 eV, which is not very different from that of CP (-6.13 eV). Thus, indicating both to exhibit better electron-donating ability. While, among the Pt(II)-DNA compounds, **4** displayed the lowest E_{HOMO} value. The difference in separation energy (E_{LUMO}-E_{HOMO}) contributes to the reactivity of chemical species. Lower the value of separation energy, higher is the reactivity to a chemical species. Molecule **1** displayed a much lower value of E_{LUMO}-E_{HOMO} energy compared to CP, thereby suggesting higher reactivity. Among the Pt(II)-DNA compounds, **5** exhibited the lowest value of separation energy, while **4** the

highest. Thus, the presence of RA non-leaving group in Pt(II)-DNA complexes resulted in a lower value the separation energy than CP.

A far as the effects of the solvent are concerned (Tables S9 and S10), one can observe that, as expected, the effect of the water is more pronounced for the molecules charged (**3** and **5**) which show enhancements of the FOs energy ranging between 2.55 and 3.54 eV. Moreover, for both gas-phase and water, no significant differences have been found comparing the values calculated with the basis sets 6-31G* and 6-311+G(d,p) (Tables S10 and S11). As a general trend one can observe that the energies of the FOs are slightly more stable (< 0.32 eV) in the case of second one, whereas HOMO-LUMO gaps and dipole moments are almost unchanged.

Further, the electronic chemical potential (μ, equation **1** in methods) can be explained as the ability of an atom in a given molecule to attract electrons and hence to work as an electrophile. In general, Pt(II)–DNA compounds displayed better ability to act as an electrophile, in agreement with the positive charge, with molecule **5** shown the lowest value of –8.34 eV (Table 4). It is interesting to note that molecule **1** displayed a better capacity to act as an electrophile than CP.

Chemical hardness (η) has been estimated from the $E_{LUMO} - E_{HOMO}$ separation energy (equation **2** in methods), which provides information on the stability of a molecule under small perturbations of a chemical reaction. Among the five molecules, **2** and **4** can be characterized as hard molecules as they have large $E_{LUMO} - E_{HOMO}$ gap, while molecule **3** and **1** as intermediate ones and **5** a soft molecule. Pt(II)-DNA compounds **2** and **4** have similar chemical hardness as CP.

On the fixed geometries of the molecules in the ground state configuration, we calculated the vertical electron affinities (EA_V) and vertical ionization energies (IE_V) using B3LYP XC functional and 6-31G* basis-set. Molecule **1** displayed higher EA_V and IE_V values than CP. From Table 4, it is apparent that molecules **5** and **3** showed values for EA_V exceeding 5 eV, while **4** less than 4 eV, and < 3 eV EA_V value for **2**. Further, for IE_V, molecule **4** displayed the most substantial value (11.78 eV), followed by while **2**, **3,** and **5**. In general, IE_V value exceeded 10.5 eV for the four Pt(II)-DNA compounds, and CP displayed the lowest value. This aspect can be related to the charge +1 of the complexes **2**-**5**, which makes it more difficult to throw out the electron in the ionization process.

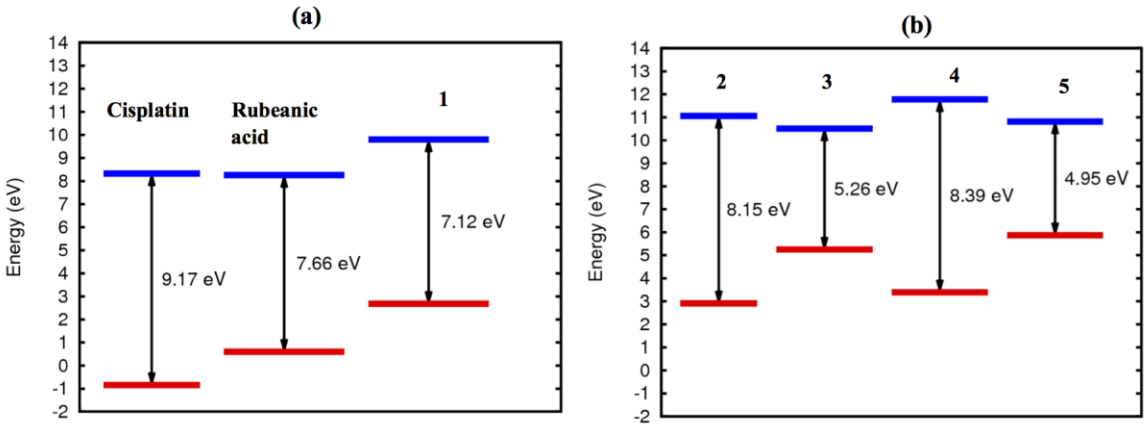

Fig. 5. Fundamental gap (E_{GAP}) for the molecules under investigation. The vertical ionization energies IE_V (blue lines), and vertical electron affinities EA_V (red lines), and fundamental gap (E_{GAP}) energy values for the five molecules are shown as black arrows.

The fundamental gap (E_{GAP}) was calculated using equation 3 (in Methods), revealed the highest E_{GAP} value of CP. However, upon substitution with the non-leaving group in CP to RA (i.e., molecule **1**) lead to a decrease in E_{GAP} by ~ 2 eV (Fig. 5a). Among the Pt(II)-DNA compounds (Fig. 5b), we found high E_{GAP} value for molecule **4** and **2** (exceeding 8 eV), and

the lowest for **5** (4.95 eV). For comparison, we repeated the calculations for all the molecules using another exchange correlation (XC) functional, i.e. PBE[56]. Between the two XC functionals (Table S12), for the fundamental gap (E_{GAP}) a maximum difference of 0.8 eV was found for cisplatin, while for molecule **1** (proposed molecule in our study) a small difference of 0.18 eV. These noted differences between the two XC functionals is indeed consistent with our previous studies [33, 34].

For completeness, additional time-dependent DFT calculations were also performed to investigate the absorption properties of the molecules. The obtained optical absorption spectra and the exciton binding energies have been provided as supplementary information.

4. Conclusions

In brief, our study reports the detailed computational investigation of molecular and electronic properties of cisplatin (CP) and molecule **1** complexes. Further, CP–, molecule **1**–DNA bases (adenine, guanine) compounds were also studied to investigate the DNA-binding capability of these systems.

Comparison of physicochemical properties between CP and molecule **1** indicated the latter to be more lipophilic, and both of them showed druglikeness characteristics. Concerning electronic properties, we found a similar pattern of HOMOs while a significant difference in the LUMOs was observed between CP and molecule **1**. This feature was consistent with the similar HOMO energy and very different LUMO energy, regular with the differences observed in the calculated electronic absorption spectra. Moreover, molecule **1** exhibited a pronounced electrophile property and higher reactivity than CP. Furthermore, similar trends in HOMOs and LUMOs energies and electronic properties were also observed between their

corresponding guanine (**2** with **3**) and adenine (**4** with **5**) complexes. Binding energy calculations revealed molecule **1** to form stable complexes with the investigated DNA bases, adhering the same stability trend of CP complexes. Altogether, the information gathered from our study indicate molecule **1** as a promising scaffold for designing compounds with improved chemotherapeutic properties.

ACKNOWLEDGEMENTS

The authors acknowledge the use of computational resources of CRS4 with special thanks to Marco Moro of HPC staffs. The authors are also grateful to Dr. Francesca Mocci, University of Cagliari, for providing the computing facility.

Compliance with ethical standards

Conflict of interest

The authors declare that they have no conflict of interest.

Electronic Supplementary Material

Optimized geometries with calculated least-square planes (Fig.s S1-S3). Bond distances of molecules (Tables S1-S7), intramolecular contacts for molecules **2-5** (Table S8) and comparisons between results obtained from different basis sets in water and gas-phase (Tables S9-S11). In Table S12, comparison between the two XC functionals (B3LYP, PBE) using the same basis set (6-31G*). HOMO−1 orbitals (Fig.S4). TD-DFT simulated electronic spectra (Fig. S5) and exciton binding energies (Fig. S6).

References

[1] T.C. Johnstone, K. Suntharalingam, S.J. Lippard, The Next Generation of Platinum Drugs: Targeted Pt(II) Agents, Nanoparticle Delivery, and Pt(IV) Prodrugs, Chem. Rev. 116 (2016) 3436-3486.
[2] G. Kemp, P. Rose, J. Lurain, M. Berman, A. Manetta, B. Roullet, H. Homesley, D. Belpomme, J. Glick, Amifostine pretreatment for protection against cyclophosphamide-induced and cisplatin-induced toxicities: results of a randomized control trial in patients with advanced ovarian cancer, J. Clin. Oncol. 14 (1996) 2101-2112.
[3] D.R. Gandara, W.A. Nahhas, M.D. Adelson, S.M. Lichtman, E.S. Podczaski, S. Yanovich, H.D. Homesley, P. Braly, P.S. Ritch, S.R. Weisberg, Randomized placebo-controlled multicenter evaluation of diethyldithiocarbamate for chemoprotection against cisplatin-induced toxicities, J. Clin. Oncol. 13 (1995) 490-496.
[4] M.J. Bloemink, J. Reedijk, Cisplatin and derived anticancer drugs: mechanism and current status of DNA binding, Met. Ions Biol. Syst. 32 (1996) 641-685.
[5] L. Giovagnini, L. Ronconi, D. Aldinucci, D. Lorenzon, S. Sitran, D. Fregona, Synthesis, Characterization, and Comparative in Vitro Cytotoxicity Studies of Platinum(II), Palladium(II), and Gold(III) Methylsarcosinedithiocarbamate Complexes, J. Med. Chem. 48 (2005) 1588-1595.
[6] D.L. Bodenner, P.C. Dedon, P.C. Keng, R.F. Borch, Effect of diethyldithiocarbamate on cis-diamminedichloroplatinum(II)-induced cytotoxicity, DNA cross-linking, and gamma-glutamyl transpeptidase inhibition, Cancer Res. 46 (1986) 2745-2750.
[7] D.W. Shen, L.M. Pouliot, M.D. Hall, M.M. Gottesman, Cisplatin resistance: a cellular self-defense mechanism resulting from multiple epigenetic and genetic changes, Pharmacol. Rev. 64 (2012) 706-721.
[8] S.W. Johnson, D. Shen, I. Pastan, M.M. Gottesman, T.C. Hamilton, Cross-resistance, cisplatin accumulation, and platinum-DNA adduct formation and removal in cisplatin-sensitive and -resistant human hepatoma cell lines, Exp. Cell Res. 226 (1996) 133-139.
[9] R.G. Pearson, Hard and Soft Acids and Bases, J. Am. Chem. Soc. 85 (1963) 3533-3539.
[10] R.T. Dorr, A Review of the Modulation of Cisplatin Toxicities by Chemoprotectants, (1996) 131-154.
[11] S. Cascinu, L. Cordella, E. Del Ferro, M. Fronzoni, G. Catalano, Neuroprotective effect of reduced glutathione on cisplatin-based chemotherapy in advanced gastric cancer: a randomized double-blind placebo-controlled trial, J. Clin. Oncol. 13 (1995) 26-32.
[12] S.E. Dible, Z.H. Siddik, F.E. Boxall, K.R. Harrap, The effect of diethyldithiocarbamate on the haematological toxicity and antitumour activity of carboplatin, Eur. J. Cancer Clin. Oncol. 23 (1987) 813-818.
[13] T.K. Schmalbach, R.F. Borch, Myeloprotective effect of diethyldithiocarbamate treatment following 1,3-bis(2-chloroethyl)-1-nitrosourea, adriamycin, or mitomycin C in mice, Cancer Res. 49 (1989) 2574-2577.
[14] C. Marzano, A. Trevisan, L. Giovagnini, D. Fregona, Synthesis of a new platinum(II) complex: anticancer activity and nephrotoxicity in vitro, Toxicol. In Vitro 16 (2002) 413-419.
[15] M.J. Cleare, J.D. Hoeschele, Anti-tumor Platinum Compounds. RELATIONSHIP BETWEEN STRUCTURE AND ACTIVITY, Platinum Met. Rev. 17 (1973) 2-13.
[16] J. Landi, N. Farrell, M.P. Hacker, Sulfoxides as leaving groups. Effect of sterically hindered aliphatic sulfoxides on the antitumor activity of chloro(substituted sulfoxide)(1,1-diaminomethylcyclohexane)platinum(II) nitrate, Inorg. Chim. Acta 202 (1992) 79-83.
[17] J.V. Burda, M. Zeizinger, J. Leszczynski, Activation barriers and rate constants for hydration of platinum and palladium square-planar complexes: An ab initio study, The Journal of Chemical Physics 120 (2004) 1253-1262.
[18] J.V. Burda, J. Šponer, J. Leszczynski, The influence of square planar platinum complexes on DNA base pairing. An ab initio DFT study, PCCP 3 (2001) 4404-4411.
[19] J.V. Burda, J. Leszczynski, How Strong Can the Bend Be on a DNA Helix from Cisplatin? DFT and MP2 Quantum Chemical Calculations of Cisplatin-Bridged DNA Purine Bases, lnorg. Chem. 42 (2003) 7162-7172.
[20] M.H. Baik, R.A. Friesner, S.J. Lippard, Theoretical study on the stability of N-glycosyl bonds: why does N7-platination not promote depurination?, J. Am. Chem. Soc. 124 (2002) 4495-4503.
[21] F. Šebesta, J.V. Burda, Study on electronic properties, thermodynamic and kinetic parameters of the selected platinum(II) derivatives interacting with guanine, J. Inorg. Biochem. 172 (2017) 100-109.
[22] W. Kohn, Nobel Lecture: Electronic structure of matter—wave functions and density functionals, Rev. Mod. Phys. 71 (1999) 1253-1266.
[23] ChemAxon.
[24] N.M. O'Boyle, M. Banck, C.A. James, C. Morley, T. Vandermeersch, G.R. Hutchison, Open Babel: An open chemical toolbox, J. Cheminform. 3 (2011) 33.

[25] A.D. Becke, Density‐functional thermochemistry. III. The role of exact exchange, J. Chem. Phys. 98 (1993) 5648-5652.
[26] C. Lee, W. Yang, R.G. Parr, Development of the Colle-Salvetti correlation-energy formula into a functional of the electron density, Physical Review B 37 (1988) 785-789.
[27] M.J. Frisch, G.W. Trucks, H.B. Schlegel, G.E. Scuseria, M.A. Robb, J.R. Cheeseman, G. Scalmani, V. Barone, B. Mennucci, G.A. Petersson, H. Nakatsuji, M. Caricato, X. Li, H.P. Hratchian, A.F. Izmaylov, J. Bloino, G. Zheng, J.L. Sonnenberg, M. Hada, M. Ehara, K. Toyota, R. Fukuda, J. Hasegawa, M. Ishida, T. Nakajima, Y. Honda, O. Kitao, H. Nakai, T. Vreven, J.A. Montgomery, J.E. Peralta, F. Ogliaro, M. Bearpark, J.J. Heyd, E. Brothers, K.N. Kudin, V.N. Staroverov, R. Kobayashi, J. Normand, K. Raghavachari, A. Rendell, J.C. Burant, S.S. Iyengar, J. Tomasi, M. Cossi, N. Rega, J.M. Millam, M. Klene, J.E. Knox, J.B. Cross, V. Bakken, C. Adamo, J. Jaramillo, R. Gomperts, R.E. Stratmann, O. Yazyev, A.J. Austin, R. Cammi, C. Pomelli, J.W. Ochterski, R.L. Martin, K. Morokuma, V.G. Zakrzewski, G.A. Voth, P. Salvador, J.J. Dannenberg, S. Dapprich, A.D. Daniels, Farkas, J.B. Foresman, J.V. Ortiz, J. Cioslowski, D.J. Fox, Gaussian 09, Revision B.01, Wallingford CT, 2009.
[28] M. Valiev, E.J. Bylaska, N. Govind, K. Kowalski, T.P. Straatsma, H.J.J. Van Dam, D. Wang, J. Nieplocha, E. Apra, T.L. Windus, W.A. de Jong, NWChem: A comprehensive and scalable open-source solution for large scale molecular simulations, Comput. Phys. Commun. 181 (2010) 1477-1489.
[29] P.J. Hay, W.R. Wadt, Ab initio effective core potentials for molecular calculations. Potentials for K to Au including the outermost core orbitals, The Journal of Chemical Physics 82 (1985) 299-310.
[30] S. Shanmugam, S. Nachimuthu, V. Subramaniam, Electronic and optical properties of edge modified peritetracene: a DFT study, Struct. Chem. (2018).
[31] R.O. Jones, O. Gunnarsson, The density functional formalism, its applications and prospects, Rev. Mod. Phys. 61 (1989) 689-746.
[32] G. Malloci, G. Cappellini, G. Mulas, G. Satta, Quasiparticle effects and optical absorption in small fullerenelike GaP clusters, Physical Review B 70 (2004).
[33] A. Kumar, R. Cardia, G. Cappellini, Electronic and optical properties of chromophores from bacterial cellulose, Cellulose 25 (2018) 2191-2203.
[34] A. Kumar, G. Cappellini, F. Delogu, Electronic and optical properties of chromophores from hexeneuronic acids, Cellulose 26 (2019) 1489-1501.
[35] X. Barril, F.J. Luque, Molecular simulation methods in drug discovery: a prospective outlook, J. Comput. Aided Mol. Des. 26 (2012) 81-86.
[36] F. Ban, K. Dalal, H. Li, E. LeBlanc, P.S. Rennie, A. Cherkasov, Best Practices of Computer-Aided Drug Discovery: Lessons Learned from the Development of a Preclinical Candidate for Prostate Cancer with a New Mechanism of Action, J. Chem. Inf. Model. 57 (2017) 1018-1028.
[37] A. Daina, O. Michielin, V. Zoete, SwissADME: a free web tool to evaluate pharmacokinetics, drug-likeness and medicinal chemistry friendliness of small molecules, Sci. Rep. 7 (2017) 42717.
[38] V.A. Levin, Relationship of octanol/water partition coefficient and molecular weight to rat brain capillary permeability, J. Med. Chem. 23 (1980) 682-684.
[39] A. Fais, B. Era, S. Asthana, V. Sogos, R. Medda, L. Santana, E. Uriarte, M.J. Matos, F. Delogu, A. Kumar, Coumarin derivatives as promising xanthine oxidase inhibitors, Int. J. Biol. Macromol. 120 (2018) 1286-1293.
[40] U. Ammarah, A. Kumar, R. Pal, N.C. Bal, G. Misra, Identification of new inhibitors against human Great wall kinase using in silico approaches, Sci. Rep. 8 (2018) 4894.
[41] A.F. Westendorf, L. Zerzankova, L. Salassa, P.J. Sadler, V. Brabec, P.J. Bednarski, Influence of pyridine versus piperidine ligands on the chemical, DNA binding and cytotoxic properties of light activated trans,trans,trans-[Pt(N3)2(OH)2(NH3)(L)], J. Inorg. Biochem. 105 (2011) 652-662.
[42] J.J. Lu, K. Crimin, J.T. Goodwin, P. Crivori, C. Orrenius, L. Xing, P.J. Tandler, T.J. Vidmar, B.M. Amore, A.G.E. Wilson, P.F.W. Stouten, P.S. Burton, Influence of Molecular Flexibility and Polar Surface Area Metrics on Oral Bioavailability in the Rat, J. Med. Chem. 47 (2004) 6104-6107.
[43] D.F. Veber, S.R. Johnson, H.-Y. Cheng, B.R. Smith, K.W. Ward, K.D. Kopple, Molecular Properties That Influence the Oral Bioavailability of Drug Candidates, J. Med. Chem. 45 (2002) 2615-2623.
[44] S. Kalepu, V. Nekkanti, Insoluble drug delivery strategies: review of recent advances and business prospects, Acta Pharmaceutica Sinica B 5 (2015) 442-453.
[45] J. Ali, P. Camilleri, M.B. Brown, A.J. Hutt, S.B. Kirton, Revisiting the General Solubility Equation: In Silico Prediction of Aqueous Solubility Incorporating the Effect of Topographical Polar Surface Area, J. Chem. Inf. Model. 52 (2012) 420-428.
[46] C.A. Lipinski, F. Lombardo, B.W. Dominy, P.J. Feeney, Experimental and computational approaches to estimate solubility and permeability in drug discovery and development settings, Adv Drug Deliv Rev 46 (2001) 3-26.

[47] A. Robertazzi, J.A. Platts, Hydrogen Bonding and Covalent Effects in Binding of Cisplatin to Purine Bases: Ab Initio and Atoms in Molecules Studies, Inorg. Chem. 44 (2005) 267-274.
[48] S. Chopra, Study of Electronic, Optical Absorption and Emission in Pure and Metal-Decorated Graphene Nanoribbons (C29H14-X; X=Ni, Fe, Ti, Co+, Al+, Cu+): First Principles Calculations, Chemphyschem 16 (2015) 1948-1953.
[49] D.H. Johnston, N.A. Miller, C.B. Tackett, cis-Diamminedichloridoplatinum(II)N,N-dimethylformamide monosolvate, Acta Crystallographica Section E Structure Reports Online 68 (2012) m863-m864.
[50] S. Lanza, G. Bruno, L. Monsù Scolaro, F. Nicolò, G. Rosace, Evidence for an unexpected chiral axis in tetraethyldithiooxamide and in its platinum(II) coordination and organometallic complexes, Tetrahedron: Asymmetry 4 (1993) 2311-2314.
[51] D.J.A. De Ridder, Structure of N,N'-dimethylpiperazine-2,3-dithione: space group correction, Acta Crystallographica Section C Crystal Structure Communications 49 (1993) 1975-1976.
[52] L. Pilia, D. Espa, A. Barsella, A. Fort, C. Makedonas, L. Marchiò, M.L. Mercuri, A. Serpe, C.A. Mitsopoulou, P. Deplano, Combined Experimental and Theoretical Study on Redox-Active d8Metal Dithione–Dithiolato Complexes Showing Molecular Second-Order Nonlinear Optical Activity, Inorg. Chem. 50 (2011) 10015-10027.
[53] M. Pavelka, J.V. Burda, Pt-bridges in various single-strand and double-helix DNA sequences. DFT and MP2 study of the cisplatin coordination with guanine, adenine, and cytosine, J. Mol. Model. 13 (2007) 367-379.
[54] G. Schröder, J. Kozelka, M. Sabat, M.-H. Fouchet, R. Beyerle-Pfnür, B. Lippert, Model of the Second Most Abundant Cisplatin−DNA Cross-Link: X-ray Crystal Structure and Conformational Analysis ofcis-[(NH3)2Pt(9-MeA-N7)(9-EtGH-N7)](NO3)·2H2O (9-MeA = 9-Methyladenine; 9-EtGH = 9-Ethylguanine), lnorg. Chem. 35 (1996) 1647-1652.
[55] H. Schoellhorn, G. Raudaschl-Sieber, G. Mueller, U. Thewalt, B. Lippert, DNA-intrastrand guanine, guanine cross-linking by cisplatin: comparison of three model compounds with head-head orientation of the nucleobases, J. Am. Chem. Soc. 107 (1985) 5932-5937.
[56] J.P. Perdew, K. Burke, M. Ernzerhof, Generalized Gradient Approximation Made Simple, Phys. Rev. Lett. 77 (1996) 3865-3868.